MiR-338-3p improved lung adenocarcinoma by *AKAP12* suppression

Jin Chang[1], Shuo Liu[2], Baowei Li[3], Zhongchao Huo[4], Xiaomin Wang[3], Hui Zhang[3]

[1]Department of Aesthetic Surgery, Affiliated Hospital of Hebei University of Engineering, Handan, Hebei, China
[2]Department of Stomatology, Handan First Hospital, Handan, Hebei, China
[3]Department of Radiology, Affiliated Hospital of Hebei University of Engineering, Handan, Hebei, China
[4]Department of Radiotherapy, Affiliated Hospital of Hebei University of Engineering, Handan, Hebei, China

Corresponding author:
Hui Zhang
Department of Radiology
Affiliated Hospital of Hebei
University of Engineering
81 Congtai Road
Handan 056002
Hebei, China
Phone: +86 0310-8572101
E-mail:
wushuming2007@126.com

Abstract

Introduction: This study aimed to explore the biological functions of *AKAP12* in lung adenocarcinoma and investigate the interaction between *AKAP12* and miR-338-3p.

Material and methods: Sixty-one differentially expressed genes in lung adenocarcinoma and adjacent normal tissues were first analyzed by TCGA. Immunohistochemistry and quantitative reverse transcription PCR (qRT-PCR) were further utilized to confirm aberrant *AKAP12* expression in tumor tissues. The influences of *AKAP12* on proliferation, invasion and migration, and apoptosis of lung adenocarcinoma were investigated by clone formation assay and MTT assay, transwell assay, and flow cytometry analysis respectively. TargetScan and miRanda databases predicted the binding sites of miRNAs on *AKAP12* 3′-UTR and structure changes were validated by RNA folding form. The target relationship between miR-338-3p and *AKAP12* was confirmed by the dual-luciferase reporter system. Disease-free survival (DFS) and overall survival (OS) curves were generated with Kaplan-Meier plotter according to the TCGA data and the correlation among *AKAP12* expression, miR-338-3p expression and prognosis was also analyzed.

Results: *AKAP12* was upregulated in lung adenocarcinoma tissues and cells (all $p < 0.01$), and negatively correlated with prognosis outcomes of patients (both $p < 0.05$). High expression of *AKAP12* promoted proliferation, invasion and migration of cancer cells, and inhibited cell apoptosis (all $p < 0.05$). MiR-338-3p could directly bind to the 3′-UTR of *AKAP12* and showed most significant suppression on *AKAP12* expression among four predicted miRNAs (all $p < 0.01$). Additionally, miR-338-3p could suppress *AKAP12* in lung adenocarcinoma, improving prognosis (all $p < 0.05$).

Conclusions: *AKAP12* acts as a tumor promoter in lung adenocarcinoma development. Upregulation of MiR-338-3p could suppress *AKAP12* expression in lung cancer cells and contribute to a better prognosis.

Key words: lung adenocarcinoma, *AKAP12*, miR-338-3p.

Introduction

Lung cancer, predominantly non-small-cell lung cancer (NSCLC), is the chief culprit for cancer mortality [1]. It is characterized by progressive metastasis and poor prognosis [2]. It is reported that lung cancer accounts for

AMS

more than one-quarter (26%) of all cancer deaths, and the 5-year survival of lung cancer is only 18% [3]. Over the past decades, targeted therapeutics have been developed against drivers of lung adenocarcinoma, a subtype of NSCLC, improving the prognosis of patients [4]. Therefore, it is essential to further explore the underlying mechanisms of lung adenocarcinoma development and develop more efficient targeted treatment.

MiRNAs widely involved in cellular processes via bind to the 3′-untranslated region (3′-UTR) of genes and regulate cell functions [5, 6]. MiR-338-3p, located on chromosome 17q25, is a miRNA which plays a critical role in promoting cell death, neuronal differentiation and neurite extension [7]. Accumulating evidence has indicated that miR-338-3p could suppress the development of various human cancers, including hepatocellular carcinoma [8], breast cancer [9] and lung cancer [10]. It plays an anti-tumor role in lung cancer, inhibiting proliferation, migration, invasion, enhancing cell apoptosis [11] and suppressing tumor metastasis [12, 13]. Several studies have reported that several oncogenes were downregulated by miR-338-3p in lung cancer, such as *IRS2* [10], *SphK2* [14] and *SOX4* [15]. Further investigation was needed to find more related genes for better understanding of lung cancer development.

AKAP12 is an A-kinase scaffold protein that possesses a characteristic binding domain for the regulatory subunit of protein kinase A [16, 17]. The loss of *AKAP12* is associated with increased cancer susceptibility [16]. *AKAP12* functions differently in various types of cancers. Xia *et al.* found that *AKAP12* was inhibited by miR-103 in hepatocellular carcinoma, thus promoting tumor growth [18]. However, other studies suggested that overexpression of *AKAP12* predicted a poor prognosis and promoted the tumor development in ovarian cancer [19] and melanoma [20]. Although evidence has highlighted that expression of *AKAP12* was closely related to cancer development, current studies on its biological function in lung cancer are limited, and the interaction between miR-338-3p and *AKAP12* also has not been determined.

In the present study, we investigated whether *AKAP12* influenced the proliferation, migration, invasion and apoptosis in lung adenocarcinoma, and examined the relationship between *AKAP12* and miR-338-3p. Our results suggested that miR-338-3p improved the prognosis of lung adenocarcinoma by suppressing *AKAP12*, providing a potential target for clinical treatment of lung adenocarcinoma.

Material and methods

Human specimens

In this study, 20 paired human lung adenocarcinoma tissues and adjacent non-tumor ones were obtained from the Affiliated Hospital of Hebei University of Engineering Hospital (Handan, China). No tissues were gained from patients who had received preoperative radiotherapy or chemotherapy before. Specimens were immediately frozen in liquid nitrogen and stored at −80°C until usage. The ethics committee of the Affiliated Hospital of Hebei University of Engineering approved this study.

Cell line and cell culture

Lung adenocarcinoma cell lines A549 and H1299 and normal human epithelial cell line HBE were purchased from BeNa Culture Collection (Beijing, China). Lung adenocarcinoma cell line A549 and normal cell line HBE were cultured in 90% Dulbecco's modified eagle medium (DMEM, Sigma, St. Louis, MO, USA) with high glucose supplemented with 10% FBS, while H1299 was maintained in Roswell Park Memorial Institute (RPMI) 1640 medium (Sigma) with 10% FBS. Cells were all cultured in 5% CO_2 at 37°C.

Bioinformatics analysis

Microarray analysis was performed with the TCGA database, and 58 adjacent tissues and 58 tumor tissues in lung adenocarcinoma were involved respectively. Differentially expressing genes were recognized by an adjusted *p*-value less than 0.05 and $\log_2$ fold change larger than 10 or less than −10. After being ranked, the ten most highly expressed genes and most lowly expressed genes were listed in Supplementary Table SI. The heat map and volcano plot were drawn with R studio.

TargetScan and miRanda were used to predict the target relationship between AKAP12 and different miRNAs. Variable scores in the above two websites were recorded as shown in Supplementary Table SII: the mirSVR score in miRanda is an estimate of the miRNA effect on the mRNA expression level. The more negative the score, the greater the effect; the PhastCons score measures the conservation of nucleotide positions and the higher the score, the stronger the conservation; the Context++ score percentile indicated the percentage of sites for the miRNA with a less favorable context++ score, which is the sum of the contribution of 14 features [21], and a higher percentile means a greater combination probability.

RNA Folding Form website was used to predict the secondary structure of mRNAs. A greater structure change indicated a greater combination probability.

Immunohistochemistry

Lung adenocarcinoma tissue sections were firstly deparaffinized and rehydrated by ethanol

Jin Chang, Shuo Liu, Baowei Li, Zhongchao Huo, Xiaomin Wang, Hui Zhang

solutions. After being washed by PBS 2-3 times, they were incubated with 3% H_2O_2 for 10 min and then were washed again with PBS. Sections were then immersed in 0.01 M citrate buffer (pH 6.0), heated by microwave at 95°C for 20 min, and cooled down at room temperature before cool water washing. They were then incubated with 3% goat serum sealant after PBS washing at room temperature for 20 min. Sections were firstly incubated overnight with primary rabbit anti-human antibody, anti-*AKAP12* (1 : 200, ab198895, Abcam, Cambridge, MA, USA) at 4°C. Then they were washed in PBS and incubated with secondary antibody, goat anti-rabbit IgG-HRP (1 : 1000, ab6721, Abcam) at room temperature for 30 min. Following the final PBS washing, they were exposed to newly prepared diaminobenzidine for 4–6 min for 15 s of hematoxylin staining, in advance of dehydration by ethanol and air drying for observation. According to the positive staining intensity in immunohistochemistry assay, we set it to be that: colorless is score 0 (–), pale yellow is score 1 (+), palm yellow and above is score 2 (++). Six fields were randomly chosen.

Cell transfection

NC mimics, miR-107 mimics, miR-613 mimics, miR-206 mimics, miR-338-3p mimics, *AKAP12*-pcDNA3.1, sh-*AKAP12*-pcDNA3.1 and pcDNA3.1 plasmid vector were all obtained from GenePharma (Shanghai, China). Before transfection, cells were incubated in a 6-well plate in 5% CO_2 at 37°C for 18–24 h. Lung adenocarcinoma cells were firstly transfected with pcDNA3.1 plasmid vector as the control, *AKAP12*-pcDNA3.1 as the *AKAP12* group, and sh-*AKAP12*-pcDNA3.1 as the sh-*AKAP12* group, respectively. Cancer cells were also transfected with 100 nM NC mimics, miR-107 mimics, miR-613 mimics, miR-206 mimics or miR-338-3p mimics respectively by Lipofectamine 2000 (Invitrogen, Carlsbad, CA, USA) according to the manufacturer's instructions. Lung adenocarcinoma cells comprised four groups: cells co-transfected with 50 nM NC mimics and 2 µg of pcDNA3.1 plasmid vector were the control group, cells co-transfected with 50 nM NC mimics and 2 µg of *AKAP12*-pcDNA3.1 were the *AKAP12* group, cells co-transfected with 50 nM miR-338-3p mimics and 2 µg pcDNA3.1 plasmid vector were the miR-338-3p mimic group, and cells co-transfected with 2 µg of *AKAP12*-pcDNA3.1 and 50 nM miR-338-3p mimics were the *AKAP12* + miR-338-3p mimic group.

Quantitative reverse transcription PCR

Total RNA was extracted from cells by TRIzol reagent (Takara Bio, Inc., Otsu, Japan). Reverse transcription of extracted RNA and real-time PCR were performed using the Reverse Transcription Kit (Takara Bio) and miRNAs qPCR Quantitation Kit (Takara Bio) according to the instructions of the manufacturer, with GAPDH as an internal control.

Table I. Sequences for RT-qPCR, PCR, siRNA and mimics

Gene	Sequence (5'-3')
q-AKAP12-F	CTGCCTTGGGAGTTTGCC
q-AKAP12-R	GGGTTACGCCTTCCCCAAG
q-GAPDH-F	ACCACAGTCCATGCCATCA
q-GAPDH-R	TCCACCACCCTGTTGCTGT
AKAP12-cDNA-F	GCTAGCTAGAGAAGTGCGGAG
AKAP12-cDNA-R	CTCGAGGTGGTACACATATGTC
AKAP12 shRNA1	CACCGCCAGAAAGGAGCCCTGAACGAATTCAGGGCTCCTTTCTGGC
AKAP12 shRNA2	CACCGCTACTCACTGTGAAGAAACGAATTTCTTCACAGTGAGTAGC
AKAP12 shRNA3	CACCGCTGAAGAATTGGTTGAAACGAATTTCAACCAATTCTTCAGC
shRNA control	CACCGCCGAAACGAGTCCGAGAACGAATTCTCGGACTCGTTTCGGC
miR-107 mimics	AGCAGCAUUGUACAGGGCUAUCA
miR-613 mimics	AGGAAUGUUCCUUCUUUGCC
miR-206 mimics	UGGAAUGUAAGGAAGUGUGUGG
miR-338-3p mimics	UCCAGCAUCAGUGAUUUUGUUG
Mimics control	UACGGGAAAUUGCUUCGCGUG

F – forward primer, R – reverse primer.

Data were analyzed by StepOne Software (Applied Biosystems, Foster City, CA, USA). The relative expression level was expressed by $2^{-\Delta\Delta C_t}$. Primers for quantitative reverse transcription PCR (qRT-PCR) were synthesized by Huada Gene (Shenzhen, China) and listed in Table I.

Western blot

Total protein was extracted using ice-cold lysis buffer (Beyotime, Shanghai, China). Proteins were separated by SDS-PAGE with an electrophoresis system (Bio-Rad, Hercules, CA, USA), and then were transferred to polyvinylidene fluoride (PVDF) membrane (Invitrogen). After being blocked with 5% skimmed milk for 4 h, the PVDF membrane was incubated with primary rabbit anti-human antibodies, anti-*AKAP12* (ab198895, 1 : 1000, Cambridge, MA, USA) and anti-GAPDH (ab9485, 1 : 2500, Cambridge, MA, USA). After incubation overnight at 4°C, the membrane was then incubated with secondary antibody, goat anti-rabbit IgG-HRP (ab6721, 1 : 2000), for 1.5 h. Protein expression was then visualized by ECL Plus Western Blotting Substrate (Thermo Scientific, Waltham, MA, USA). The concentration of proteins was quantified by Quantity One Software (Bio-Rad).

Clone formation assay

Cells were seeded in plates (200–300 cells per plate) and incubated in 5% CO_2 at 37°C for 1–2 weeks until cell colonies were visible. After PBS washing, they were fixed with 4% paraformaldehyde for 15 min and stained with 0.1% crystal violet for observation. Finally, clone number was quantified with a microscope.

MTT assay

Approximately 2×10^3 cells were seeded into 96-well plates for 3–5 days of incubation after suspension. Then 10 μl of MTT (5 mg/ml, Sigma) was added into each well for another 4 h of incubation. Supernatants were removed and 100 μl of dimethyl sulfoxide (DMSO, Sigma) was added to each well for 10 min shaking. Then the absorbance (optical density) was measured at 490 nm on a microplate reader (Molecular Devices, Sunnyvale, CA, USA).

Transwell assay

The upper chamber of a transwell chamber (Costar, Corning Inc., Corning, NY, USA) was plated with approximately 1×10^5 cells without serum, while the lower chamber was plated with 800 μl of culture medium (5 mg/l fibronectin and 10% FBS). After incubation at 37°C in 5% CO_2 for 24 h, non-invading cells were removed from the upper chamber. Three independent fields were selected to observe hematoxylin and eosin stained bottom cells.

Flow cytometry (FCM) analysis

Transfected lung adenocarcinoma cells A549 and H1299 were incubated for 48 h, and then stained with a FITC Annexin V Apoptosis Detection Kit (BD Biosciences, Bedford, MA, USA). Then cells were subjected to apoptosis detection by FACSCalibur FCM (BD Biosciences). The data were analyzed by the software FACS Diva (BD Biosciences).

Dual-luciferase reporter system

Plasmid vector psiCHECK2 was purchased from Promega (Madison, WI, USA). 3′UTR sequences of wild-type (WT) and mutant-type (MT) *AKAP12* were inserted into the cleavage sites of the psiCHECK2 vector. PsiCHECK2-UTR vectors, negative mimics and miR-338-3p mimics were transfected into cancer cells using Lipofectamine 2000 (Invitrogen). Firefly and Renilla luciferase activities were measured 48 h later using the Dual-Luciferase Reporter System (Promega).

Statistical analysis

Data in this study were analyzed by GraphPad Prism 6.0 (Intuitive Software for Science, San Diego, CA, USA). Values were mean ± standard deviation. Two groups were compared with Student's *t* test, while multiple groups were compared using one-way ANOVA. All experiments were independently performed at least three times. The value of $p < 0.05$ was considered statistically significant.

Results

AKAP12 was highly expressed in lung adenocarcinoma

According to the TCGA analysis, 61 genes in total were selected for their aberrant expression in lung adenocarcinoma tissues ($n = 58$) compared with normal tissues ($n = 58$). Then 10 high-expressed genes and 10 low-expressed genes were listed in Supplementary Table SI and heatmap and volcano plots were drawn in Figure 1 A. *AKAP12,* a confusing gene which functioned differently in different cancers, was found overexpressing in lung adenocarcinoma tissues. Analyzed with Kaplan-Meier method, high expression of *AKAP12* contributed to worse prognosis regarding shorter disease free survival time (DFS) and overall survival time (OS) ($p < 0.01$, Figure 1 B). Immunohistochemical staining was performed in 20 paired lung carcinoma tissues and adjacent normal tissues. The staining value for each sample was presented in Supple-
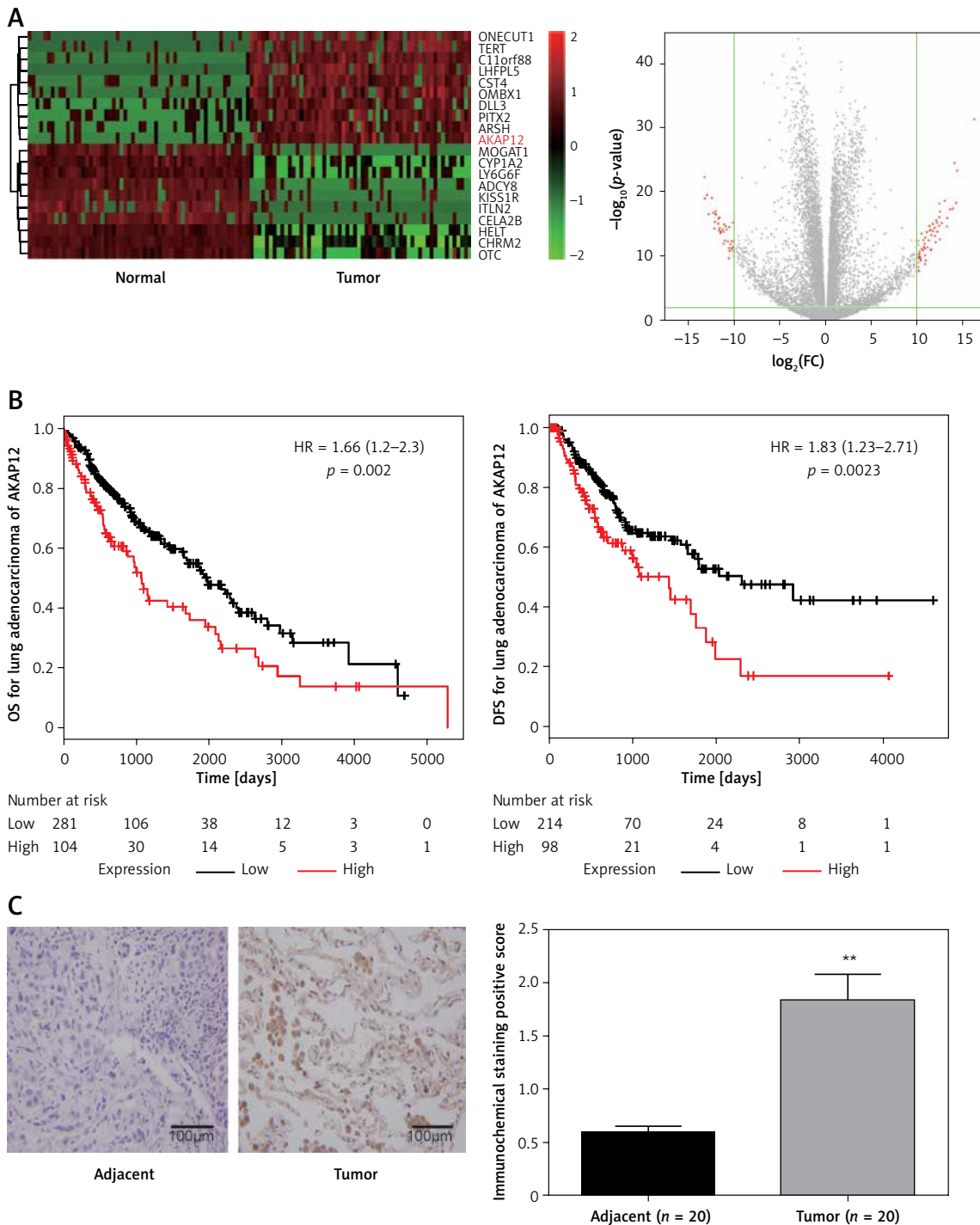
Jin Chang, Shuo Liu, Baowei Li, Zhongchao Huo, Xiaomin Wang, Hui Zhang

Figure 1. *AKAP12* was highly expressed in lung adenocarcinoma tissues. **A** – Heat map and volcano plot for 20 genes in lung adenocarcinoma. *AKAP12* was highly expressed in tumor tissues. **B** – *AKAP12* high expression resulted in worse prognosis. Low expression of *AKAP12* significantly lengthened the overall survival time (OS) and disease-free survival time (DFS). **C** – Immunohistochemistry chart for *AKAP12*. *AKAP12* was highly expressed in tumor tissues compared with adjacent ones regarding immunochemical staining positive score

mentary Table SIII and the AKAP12 staining value was higher in tumor tissues (average score = 1.84) compared with normal tissues (average score = 0.60) (Figure 1 C). The aberrantly high expression of AKAP12 could be a potential factor to promote the development of lung adenocarcinoma.

Up-regulation of *AKAP12* deteriorated lung adenocarcinoma in functional experiments

To further investigate the role of *AKAP12* in lung adenocarcinoma, we utilized qRT-PCR and Western blot assay and confirmed that both the

mRNA and protein level of AKAP12 were higher in cancer cell lines A549 and H1299 compared to the normal cell line HBE (all *p* < 0.01, Figure 2 A). Transient transfection was performed in both A549 and HBE cells using pcDNA3.1 vector, pcDNA3.1-AKAP12 cDNA or pcDNA3.1-AKAP12 shRNA. At 48 h after transfection, cells were collected and the biological functions were detected. According to the clone formation assay, cell proliferation was significantly upregulated in the *AKAP12* group while it was downregulated in the *AKAP12* shRNA group (Figure 2 B). Also, cell viability detected by MTT assay in A549 and H1299 cells with overexpression of *AKAP12* both displayed an increase (all *p* < 0.05, Figures 2 C, D). Therefore, *AKAP12* overexpression could significantly promote cell proliferation and cell viability, and vice versa. As shown in Figure 3 A, *AKAP12* overexpression could dramatically accelerate cell invasion while its suppression could inhibit cell invasion (all *p* < 0.01). The wound healing assay also displayed a similar trend: at the 24th h after the scratch, more migration appeared in the *AKAP12* overexpression group but less migration in the *AKAP12* suppression group (*p* < 0.01, *p* < 0.001, Figure 3 B). As expected, the cell apoptosis rate was significantly downregulated in the *AKAP12* group and was upregulated in the *AKAP12* shRNA group, confirming that *AKAP12* suppressed cell apoptosis and led to deterioration of lung adenocarcinoma (*p* < 0.05, *p* < 0.01, *p* < 0.001, Figure 3 C).

AKAP12 was the target of miR-338-3p and could be down-regulated by miR-338-3p

By TargetScan 7.0 and miRNA base selection, four miRNAs significantly regulated *AKAP12* in terms of bioinformatics. MiR-107 directly targeted site 57, miR-206 site 520, miR-613 site 522, and miR-338-3p site 864 (Figures 4 A, B). Different effects were judged from mirSVR score, PhastCons score, and context++ score percentile as suggested in Supplementary Table SII. MiR-338-3p had the lowest mirSVR score and a relatively high PhastCons score, indicating the highest thermal stability and a relatively good conservativeness. MiR-338-3p also had the highest context++ score, suggesting the greatest conservation and mRNA destabilization. Therefore, miR-338-3p could be the most suitable candidate for the target gene. Also, *AKAP12* structure mutations were predicted according to the RNA Folding Form website, which showed the most significant changes in the miR-338-3p group (Figure 4 C and Supplementary Figures S1–S4). After transfection of 100 nM miRNAs into HEK 293T cells, different effects of four miRNAs on *AKAP12* expression were confirmed in Figure 4 D by qRT-PCR detection, and miR-338-3p resulted in the most significant decrease in *AKAP12*

mRNA expression (both *p* < 0.01). Scores, structure changes and mRNA level changes of *AKAP12* combined confirmed that miR-338-3p could drastically downregulate *AKAP12* expression and miR-338-3p was selected as a topic. Then, luciferase activity of the control group, NC mimic group and miR-338-3p mimic group revealed that miR-338-3p directly targeted *AKAP12* and downregulated its expression (Figure 4 E).

MiR-338-3p could inhibit lung adenocarcinoma by *AKAP12* suppression

To further understand the effect of miR-338-3p on *AKAP12* expression, cells transfected with different plasmids or sequences were divided into four groups, i.e. the control group, AKAP12 group, miR-338-3p mimic group and *AKAP12* + miR-338-3p mimic group. *AKAP12* significantly upregulated *AKAP12* mRNA expression while miR-338-3p downregulated it, but *AKAP12* and miR-338-3p combined caused no significant differences (*p* < 0.05, Figure 5 A). *AKAP12* protein expression was upregulated in the *AKAP12* group and downregulated in the miR-338-3p group, but showed no significant differences in the *AKAP12* + miR-338-3p mimic group (*p* < 0.05, Figure 5 B). Also, after dividing the patients into two groups according to the median miR-338-3p expression, we found that high expression of miR-338-3p would improve the prognosis, considering the higher DFS and OS rates (Figures 5 C, D). With the Kaplan-Meier method and Cox regression models, univariate and multivariate analysis for the overall survival of lung adenocarcinoma was performed using the data from the TCGA database (Tables II and III). Stage event pathologic stage (I–IV), M stage, miR-388-3p and *AKAP12* expression were all correlated with the prognosis in univariate analysis while both miR-388-3p and *AKAP12* expression were recognized as independent prognostic factors for the overall survival. The above results verified that miR-338-3p suppressed the progression of lung adenocarcinoma by inhibiting *AKAP12*.

Discussion

Our study indicated that the expression level of *AKAP12* was high in lung adenocarcinoma. Meanwhile, high expression of *AKAP12* predicted a poor prognosis. *AKAP12* alpha previously was reported to be a promoter in lung cancer in the research of Jo *et al.*; *AKAP12*α protein was downregulated in H358, H460 and Calu-1 cells but not H1299 cells, which to a degree is consistent with this study. The methylation status of 5′CpG islands of the *AKAP12*α gene in lung tissues might be the reason for the promotion [17]. *AKAP12*, which was methylated at nearly 40% prevalence in lung ade-

Jin Chang, Shuo Liu, Baowei Li, Zhongchao Huo, Xiaomin Wang, Hui Zhang
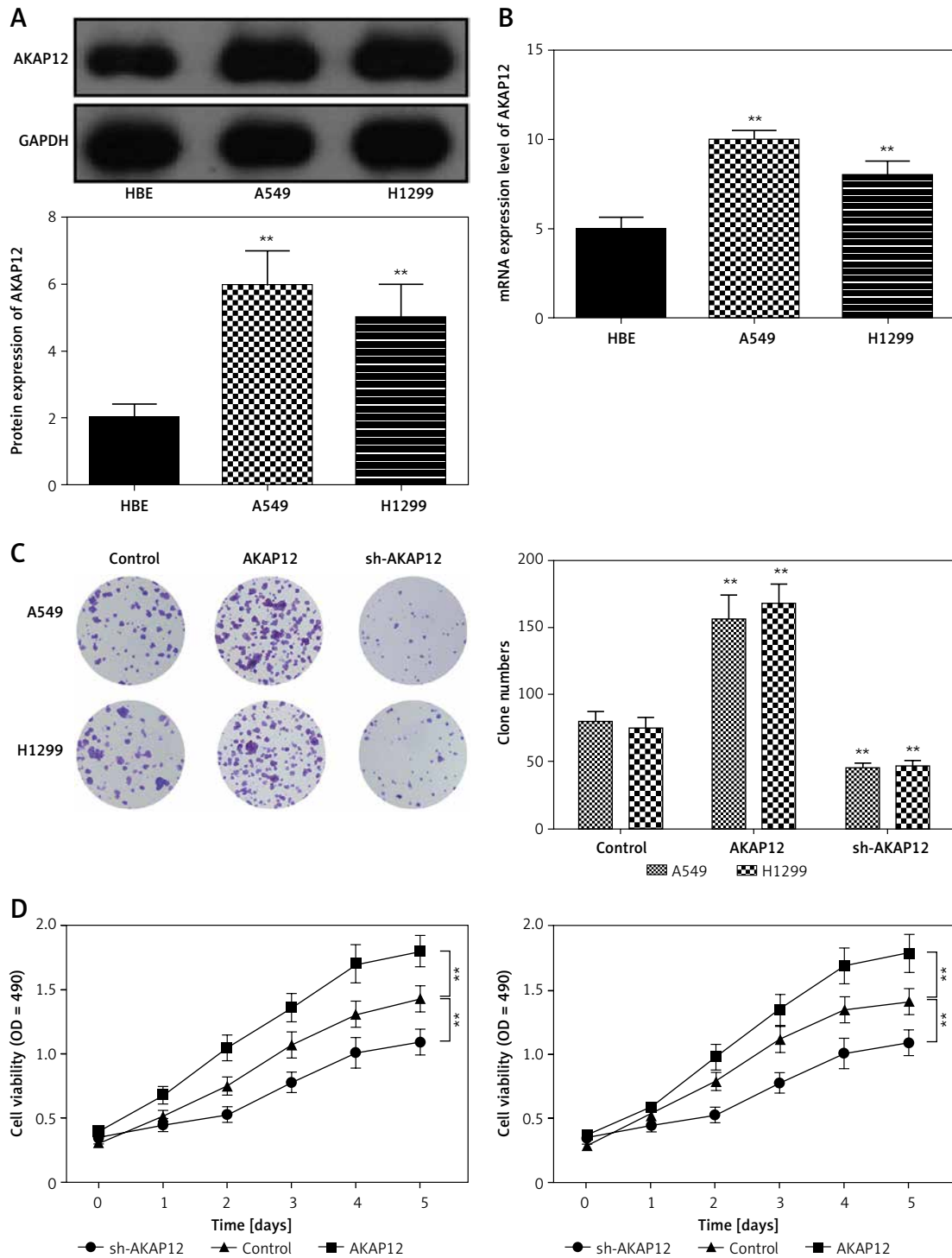

Figure 2. *AKAP12* was highly expressed in lung adenocarcinoma cells. **A** – *AKAP12* was highly expressed in A549 and H1299 cells in protein level. **B** – *AKAP12* was highly expressed in A549 and H1299 cells in mRNA level. **C** – Clone formation revealed that *AKAP12* could promote A549 and H1299 cell proliferation and its knockdown could inhibit proliferation. **D** – MTT assay revealed that *AKAP12* significantly increased cell viability while sh-*AKAP12* decreased cell viability

**p < 0.01, compared with control group.

nocarcinoma samples and modulates the expression of genes involved in the cell cycle and apoptosis, was not associated with age at diagnosis or stage of lung cancer [22]. This study by contrast proved a relationship between *AKAP12* and DFS as well as OS, which hallmarked its biomarker role in lung adenocarcinoma prognosis. After manipulating the expression of *AKAP12* in A549 and
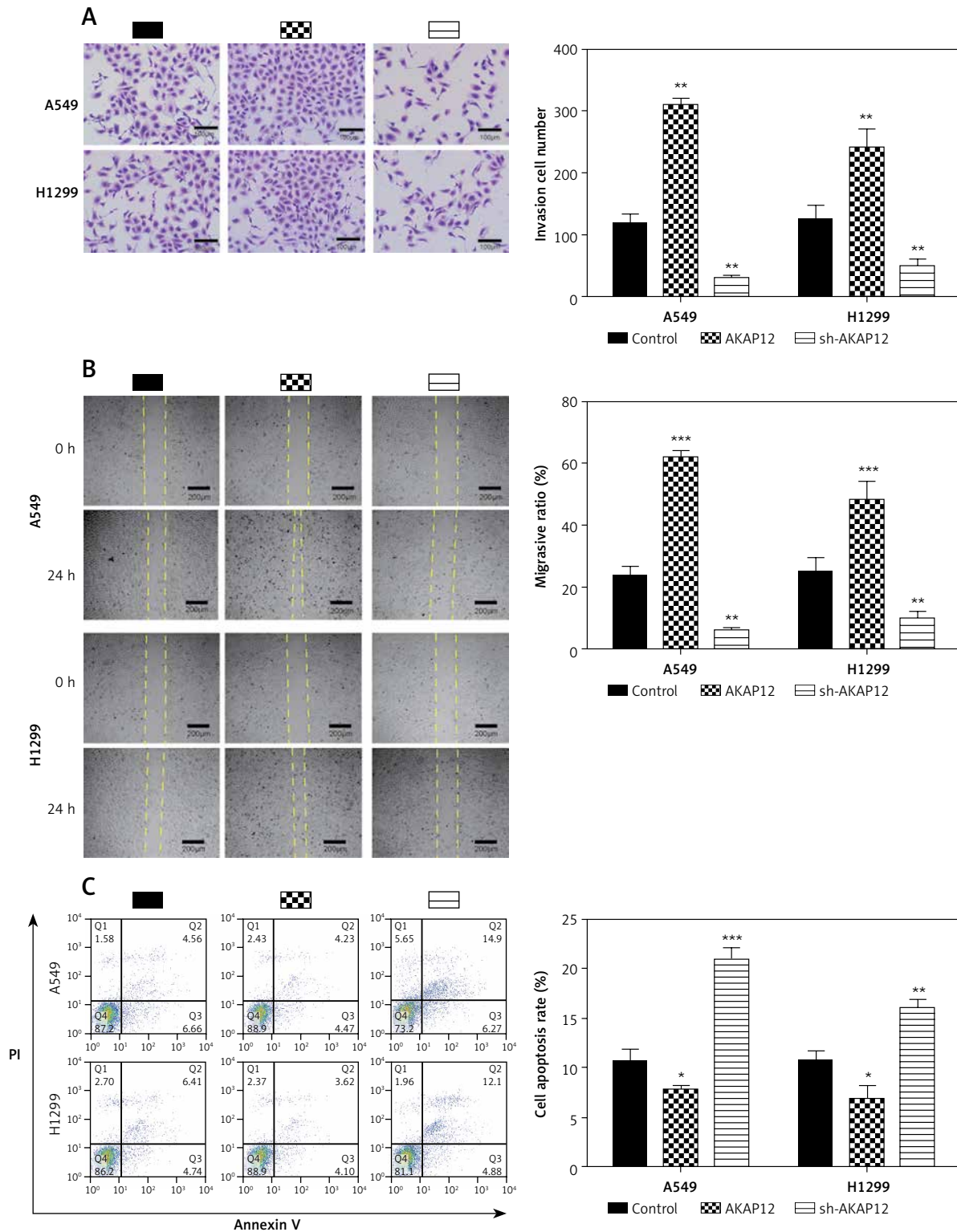
Figure 3. *AKAP12* deteriorated lung adenocarcinoma in functional experiments. **A** – Transwell assay revealed that *AKAP12* could increase cell invasion and its knockdown could inhibit the process. **B** – Wound healing assay revealed that *AKAP12* could improve migration ratio and its knockdown could decrease the ratio. **C** – Flow cytometry revealed that *AKAP12* could reduce cell apoptosis rate and its knockdown could increase cell apoptosis rate

*$p < 0.05$, **$p < 0.01$, ***$p < 0.001$, compared with control group.

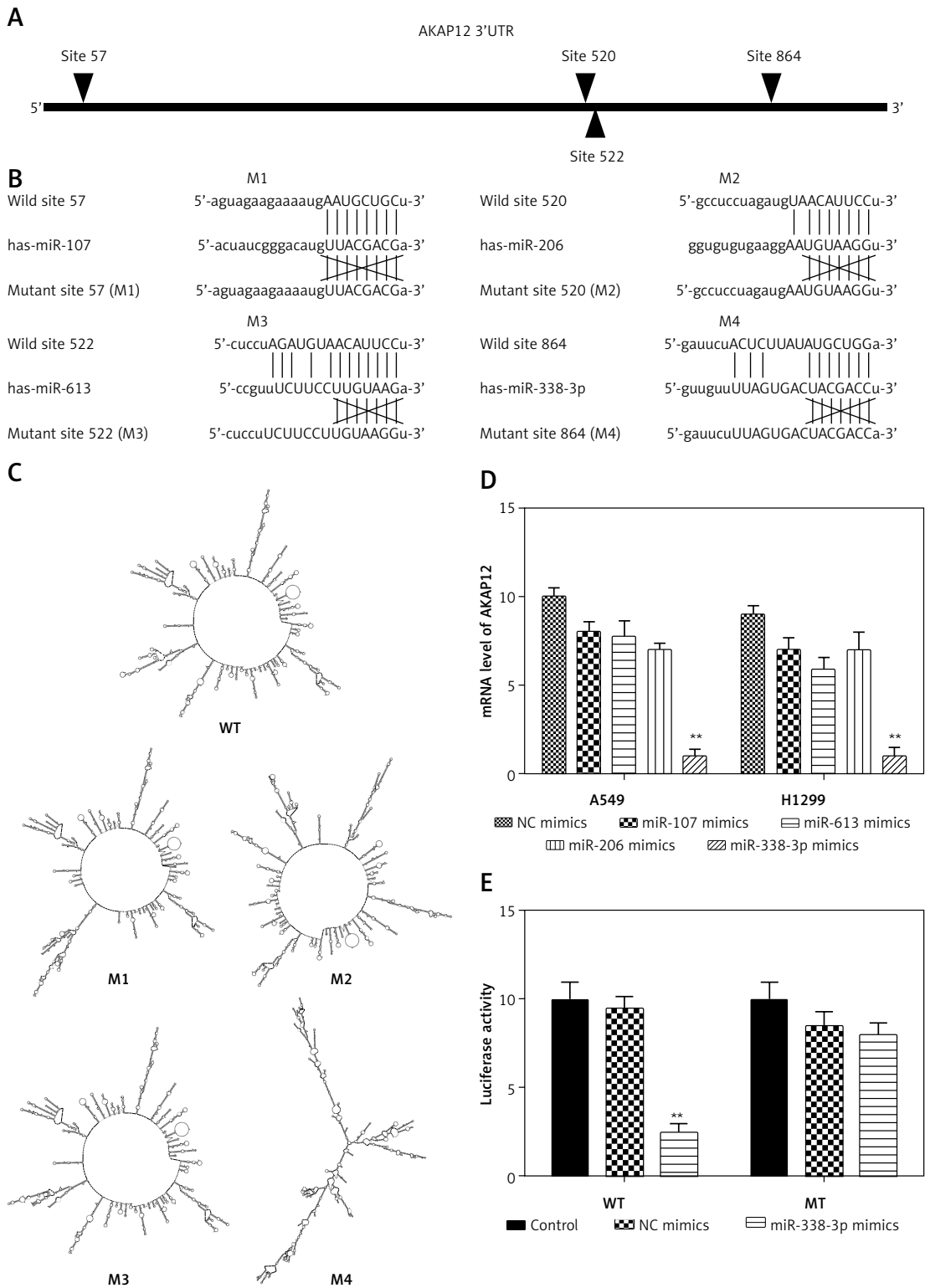Jin Chang, Shuo Liu, Baowei Li, Zhongchao Huo, Xiaomin Wang, Hui Zhang

Figure 4. *AKAP12* was the target of miR-338-3p and could be down-regulated by miR-338-3p. **A** – Targeted sites of four miRNAs are displayed. MiR-107 targeted at site 57, miR-206 at site 520, miR-613 at site 522, and miR-338-3p at site 864. **B** – Four miRNAs all directly targeted at *AKAP12* instead of its variants. **C** – Structures changes after miRNAs combination according to RNA folding form 23.0. *AKAP12* mutant 4 had significant structure changes caused by miR-338-3p. **D** – Q-PCR of four miRNAs revealed that four miRNAs could downregulate *AKAP12* expression, and miR-338-3p displayed the most significant changes. **E** – MiR-338-3p could inhibit the luciferase activity of WT 3'UTR of *AKAP12* but had little influence on MT 3'UTR of *AKAP12*

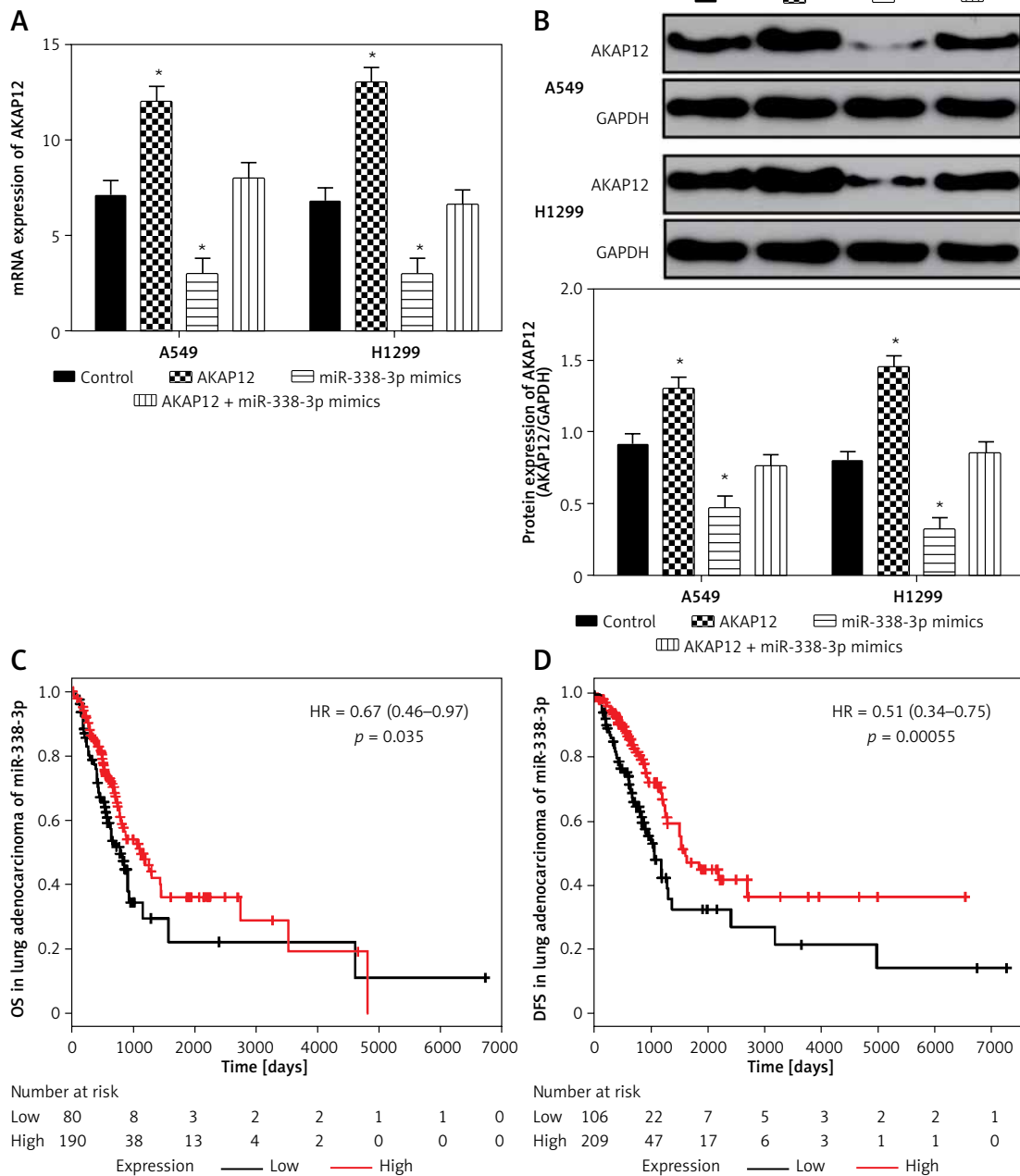***p < 0.01, compared with control group.*

Figure 5. MiR-338-3p inhibited lung adenocarcinoma by *AKAP12* suppression. **A, B** – MiR-338-3p could down-regulate the expression of *AKAP12* according to qRT-PCR and western blot. **C, D** – MiR-338-3p high expression led to better DFS and OS

*p < 0.05, compared with control group.

H1299 cells, we confirmed that *AKAP12* acts as an oncogene and facilitated the proliferation, migration and invasion of lung cancer cells.

The promotion effect of *AKAP12* on lung adenocarcinoma was associated with miR-338-3p as we proved the target relationship between miR-338-3p and *AKAP12*. MiR-338 was reported to abate lung cancer *in vitro* and *in vivo* by targeting *ITGB3* [13], a conclusion similar to this study. MiR-338-3p could suppress lung cancer tumorigenesis and metastasis *in vitro* and *in vivo* by targeting the EMT regulator Sox4 as well [9]. MiR-338-3p

was also predicted in an integrative bioinformatics analysis as a biomarker for diagnosis of NSCLC adenocarcinoma [23]. In this research, miR-338-3p was discovered to target *AKAP12* and inhibited lung adenocarcinoma development, which to our knowledge had not been studied before. As a result, our study demonstrated a new regulatory mechanism of miR-338-3p, which revealed a better strategy for lung adenocarcinoma treatment.

However, there are some limitations in this study. The underlying mechanisms of *AKAP12* regulation in lung adenocarcinoma remains to be

Jin Chang, Shuo Liu, Baowei Li, Zhongchao Huo, Xiaomin Wang, Hui Zhang

Table II. Univariate analysis for overall survival

Factors	β	HR (95% CI for HR)	*P*-value
Age	−0.03964	0.9611 (0.7727–1.196)	0.7218
Gender	0.04459	1.046 (0.8558–1.278)	0.6626
Location in lung parenchyma	−0.3242	0.7231 (0.5042–1.037)	0.07671
Targeted molecular therapy	0.05719	1.059 (0.6697–1.674)	0.8067
Radiation therapy	−0.04471	0.9563 (0.4826–1.895)	0.898
Stage event pathologic stage	−0.3167	0.7285 (0.5545–0.9573)	0.02244*
T stage	0.0185	1.019 (0.7429–1.397)	0.9085
N stage	−0.2032	0.8161 (0.6086–1.094)	0.1739
M stage	−0.3755	0.687 (0.5525–0.8541)	0.000679*
Tobacco smoking history	−0.07018	0.9322 (0.7598–1.144)	0.5011
miR-338-3p	0.2738	1.315 (1.051–1.645)	0.01636*
AKAP12	−0.2867	0.7507 (0.6032–0.9344)	0.009983*

HR – hazard radio for death. Stage event pathologic stage includes stages I–IV. *p < 0.05 indicates statistical significance.

Table III. Multivariate analysis for overall survival of AKAP12 and miR-338

Factors	HR (95% CI for HR)	*P*-value
Stage event pathologic stage	0.781 (0.5917–1.0308)	0.0809
M stage	0.6805 (0.5446–0.8502)	7.00E-04
SELE	1.4344 (1.1398–1.8052)	0.0021
TLX2	0.7101 (0.5682–0.8876)	0.0026

HR – hazard radio for death. Stage event pathologic stage included stages I–IV. *p < 0.001 indicates statistical significance.

further investigated including methylation and phosphorylation. *AKAP12*α and *AKAP12*β expression and corresponding results still need exploration as well as in the case of opposite results when it comes to lung adenocarcinoma. MiRNAs which may have better combination with *AKAP12* could be discussed in future studies for the consideration of better application in lung adenocarcinoma treatment.

In conclusion, *AKAP12* was upregulated in lung adenocarcinoma, and its high expression promoted tumor development and predicted poor prognosis. High expression of *AKAP12* in lung adenocarcinoma led to proliferation, migration and invasion of cancer cells, and apoptosis inhibition. MiR-338-3p directly targeted *AKAP12* and inhibited lung adenocarcinoma by *AKAP12* restraint. The regulation of miR-338-3p and *AKAP12* could be of value for clinic targeted therapy of lung adenocarcinoma.

Conflict of interest

The authors declare no conflict of interest.

References

1. Siegel RL, Miller KD, Jemal A. Cancer statistics, 2016. CA Cancer J Clin 2016; 66: 7-30.
2. Wu KL, Tsai MJ, Yang CJ, et al. Liver metastasis predicts poorer prognosis in stage IV lung adenocarcinoma patients receiving first-line gefitinib. Lung Cancer 2015; 88: 187-94.
3. Siegel RL, Miller KD, Jemal A. Cancer statistics, 2017. CA Cancer J Clin 2017; 67: 7-30.
4. de Langen AJ, Smit EF. Therapeutic approach to treating patients with BRAF-mutant lung cancer: latest evidence and clinical implications. Ther Adv Med Oncol 2017; 9: 46-58.
5. Lujambio A, Lowe SW. The microcosmos of cancer. Nature 2012; 482: 347-55.
6. Krol J, Loedige I, Filipowicz W. The widespread regulation of microRNA biogenesis, function and decay. Nat Rev Genet 2010; 11: 597-610.
7. Kos A, Olde Loohuis NF, Wieczorek ML, et al. A potential regulatory role for intronic microRNA-338-3p for its host gene encoding apoptosis-associated tyrosine kinase. PLoS One 2012; 7: e31022.
8. Wang G, Sun Y, He Y, Ji C, Hu B, Sun Y. MicroRNA-338-3p inhibits cell proliferation in hepatocellular carcinoma by target forkhead box P4 (FOXP4). Int J Clin Exp Pathol 2015; 8: 337-44.

9. Jin Y, Zhao M, Xie Q, Zhang H, Wang Q, Ma Q. Micro-RNA-338-3p functions as tumor suppressor in breast cancer by targeting SOX4. Int J Oncol 2015; 47: 1594-602.

10. Zhang P, Shao G, Lin X, Liu Y, Yang Z. MiR-338-3p inhibits the growth and invasion of non-small cell lung cancer cells by targeting IRS2. Am J Cancer Res 2017; 7: 53-63.

11. Sun J, Feng X, Gao S, Xiao Z. microRNA-338-3p functions as a tumor suppressor in human nonsmallcell lung carcinoma and targets Ras-related protein 14. Mol Med Rep 2015; 11: 1400-6.

12. Hong-Yuan W, Xiao-Ping C. miR-338-3p suppresses epithelial-mesenchymal transition and metastasis in human nonsmall cell lung cancer. Indian J Cancer 2015; 52 Suppl 3: E168-71.

13. Chen X, Wei L, Zhao S. miR-338 inhibits the metastasis of lung cancer by targeting integrin beta3. Oncol Rep 2016; 36: 1467-74.

14. Zhang G, Zheng H, Zhang G, et al. MicroRNA-338-3p suppresses cell proliferation and induces apoptosis of non-small-cell lung cancer by targeting sphingosine kinase 2. Cancer Cell Int 2017; 17: 46.

15. Li Y, Chen P, Zu L, Liu B, Wang M, Zhou Q. Micro-RNA-338-3p suppresses metastasis of lung cancer cells by targeting the EMT regulator Sox4. Am J Cancer Res 2016; 6: 127-40.

16. Hayashi M, Nomoto S, Kanda M, et al. Identification of the A kinase anchor protein 12 (AKAP12) gene as a candidate tumor suppressor of hepatocellular carcinoma. J Surg Oncol 2012; 105: 381-6.

17. Jo UH, Whang YM, Sung JS, Kim YH. Methylation of AKAP12{alpha} promoter in lung cancer. Anticancer Res 2010; 30: 4595-600.

18. Xia W, Ni J, Zhuang J, Qian L, Wang P, Wang J. MiR-103 regulates hepatocellular carcinoma growth by targeting AKAP12. Int J Biochem Cell Biol 2016; 71: 1-11.

19. Bateman NW, Jaworski E, Ao W, et al. Elevated AKAP12 in paclitaxel-resistant serous ovarian cancer cells is prognostic and predictive of poor survival in patients. J Proteome Res 2015; 14: 1900-10.

20. Finger EC, Castellini L, Rankin EB, et al. Hypoxic induction of AKAP12 variant 2 shifts PKA-mediated protein phosphorylation to enhance migration and metastasis of melanoma cells. Proc Natl Acad Sci USA 2015; 112: 4441-6.

21. Riffo-Campos AL, Riquelme I, Brebi-Mieville P. Tools for sequence-based miRNA target prediction: what to choose? Int J Mol Sci 2016; 17. pii: E1987.

22. Tessema M, Belinsky SA. Mining the epigenome for methylated genes in lung cancer. Proc Am Thorac Soc 2008; 5: 806-10.

23. Shao Y, Liang B, Long F, Jiang SJ. Diagnostic microRNA biomarker discovery for non-small-cell lung cancer adenocarcinoma by integrative bioinformatics analysis. Biomed Res Int 2017; 2017: 2563085.